*Laser and Particle Beams*

**cambridge.org/lpb**

# Laser-driven acceleration of heavy ions at ultra-relativistic laser intensity

J. Domański[1], J. Badziak[1] and M. Marchwiany[2]

[1]Institute of Plasma Physics and Laser Microfusion, Warsaw, Poland and [2]Interdisciplinary Centre for Mathematical and Computational Modelling, University of Warsaw, Warsaw, Poland

## Research Article

**Cite this article:** Domański J, Badziak J, Marchwiany M (2018). Laser-driven acceleration of heavy ions at ultra-relativistic laser intensity. *Laser and Particle Beams* **36**, 507–512. https://doi.org/10.1017/S0263034618000563

Received: 7 November 2018
Accepted: 10 December 2018

**Key words:**
heavy ion beam; laser-driven ion acceleration; laser–plasma interaction; multi-PW laser

**Author for correspondence:**
J. Domański, Institute of Plasma Physics and Laser Microfusion, Warsaw, Poland, E-mail: jaroslaw.domanski@ifpilm.pl

## Abstract

This paper presents the results of numerical investigations into the acceleration of heavy ions by a multi-PW laser pulse of ultra-relativistic intensity, to be available with the Extreme Light Infrastructure lasers currently being built in Europe. In the numerical simulations, performed with the use of a multi-dimensional (2D3V) particle-in-cell code, the thorium target with a thickness of 50 or 200 nm was irradiated by a circularly polarized 20 fs laser pulse with an energy of ~150 J and an intensity of $10^{23}$ W/cm$^2$. It was found that the detailed run of the ion acceleration process depends on the target thickness, though in both considered cases the radiation pressure acceleration (RPA) stage of ion acceleration is followed by a sheath acceleration stage, with a significant role in the post-RPA stage being played by the ballistic movement of ions. This hybrid acceleration mechanism leads to the production of an ultra-short (sub-picosecond) multi-GeV ion beam with a wide energy spectrum and an extremely high intensity (>$10^{21}$ W/cm$^2$) and ion fluence (>$10^{17}$ cm$^{-2}$). Heavy ion beams of such extreme parameters are hardly achievable in conventional RF-driven ion accelerators, so they could open the avenues to new areas of research in nuclear and high energy density physics, and possibly in other scientific domains.

## Introduction

High-peak-power lasers operating currently are capable of generating sub-picosecond light pulses of PW power and intensity approaching $10^{21}$–$10^{22}$ W/cm$^2$ (Danson *et al.*, 2015). Extreme Light Infrastructure (ELI), being under construction in the Czech Republic (ELI-Beamlines), Romania (ELI-Nuclear Physics), and Hungary (ELI-ALPS), will be the first laser infrastructure enabling the production of multi-PW light pulses with intensities from the ultra-relativistic intensity region (light intensities ≥$10^{23}$ W/cm$^2$) (Negoita *et al.*, 2016; http://www.eli-laser.eu). One of the primary missions of ELI consists in producing a new generation of laser-driven sources of ion beams with unique parameters hardly attainable in conventional RF-driven ion accelerators (Negoita *et al.*, 2016; http://www.eli-laser.eu). Such ion beams could open an avenue to a new area of application of high-energy ions in nuclear and particle physics, high energy density physics (HEDP) or materials science.

For applications in nuclear physics and HEDP, especially useful are energetic beams of heavy and super-heavy ions (with an atomic mass number $A > 200$) (Hoffmann *et al.*, 2009; Negoita *et al.*, 2016; Sharkov *et al.*, 2016). In particular, the use of such ion beams for research in these fields is one of the primary goals of the ELI-NP. The key topic of the ELI-NP research program, of great importance for nuclear astrophysics, is to study the production of neutron-rich heavy nuclei by a new reaction mechanism called fission–fusion using high-energy thorium ($^{232}$Th) ion beams (Negoita *et al.*, 2016). In the universe, nuclei lighter than iron are produced inside the stars as an effect of fusion processes. Heavier elements could be produced *via* the slow neutron capture process (s-process) inside the adiabatic giant branch (AGB) stars, or *via* the rapid neutron capture process (r-process) in supernova explosions, or through mergers of neutron stars. The knowledge of the properties of neutron-rich heavy nuclei produced by the r-process is crucial for understanding of this process and could bring us closer to understanding the nature of the creation of heavy elements in the universe. The proposed fission–fusion mechanism requires thorium ion beams with an energy per nucleon of 7 MeV (the thorium ion energy of 1.6 GeV), fluencies $F_i \sim 10^{18}$ cm$^{-2}$, ion beam intensities $I_i \sim 10^{20}$ W/cm$^2$, and the total number of thorium ions $N_i \sim 10^{11}$ (Negoita *et al.*, 2016). Such ion beam parameters are unattainable in conventional accelerators, so conducting research of this kind has been impossible so far. The production of super-heavy ion beams with such parameters is basically possible to attain using a laser-driven accelerator with a multi-PW laser driver.

In contrast to the laser acceleration of light ions, which has been studied extensively for many years (see, for example, the review papers by Daido *et al.*, 2012 and Macchi *et al.*, 2013), the acceleration of heavy ions has been investigated to a much lesser extent, and the investigations, both experimental and numerical ones, have been conducted in the range of laser intensities



CAMBRIDGE UNIVERSITY PRESS

$<10^{22}$ W/cm$^2$ (Clark *et al.*, 2000; Badziak *et al.*, 2001; Badziak *et al.*, 2003; McKenna *et al.*, 2004; Flippo *et al.*, 2007; Wu *et al.*, 2014; Nishiuchi *et al.*, 2015; Petrov *et al.*, 2016). However, the acceleration of heavy or super-heavy ions to GeV or multi-GeV energies, desirable in the majority of applications, requires higher, ultra-relativistic laser intensities ($\sim 10^{23}$ W/cm$^2$ or higher), which will be achievable only when the multi-PW ELI lasers (or others) are launched. Presently, only theoretical and numerical studies of the acceleration of such ions in the ultra-relativistic intensity regime are possible. They are a necessary step toward understanding the basic properties of ion acceleration in this regime, and to prepare experiments with multi-PW lasers at large laser facilities such as ELI.

Heavy ions, and especially the super-heavy ones, have certain specific features that differentiate them significantly from light ions. First of all, they have a very high ion charge state, which leads to a very high electron density in the ionized target and can be a reason for a Coulomb explosion of ions (which can affect the ion acceleration process). Second, they have a small $z/A$ ratio, typically much less than 1/3. As a result, the efficiency of ion acceleration can be significantly lower than for protons ($z/A = 1$) or light ions ($z/A \sim ½$). Finally, the high inertia of ions, which can cause the ballistic movement of ions, can significantly affect the acceleration process. So, we can expect that the mechanism of acceleration and parameters of generated ion beams can be different from those of light ions. For these reasons, detailed studies of the process of heavy and super-heavy ion acceleration, especially in the ultra-relativistic intensity regime, are necessary in order to produce ion beams with parameters useful for applications.

In this paper we investigate the acceleration of thorium ions by a multi PW laser pulse with parameters corresponding to those of the ELI-NP lasers, using numerical particle-in-cell (PIC) simulations. The main focus is placed on studying the mechanism of acceleration of super-heavy ions and testing the possibility of producing thorium ion beams with the parameters required for the fission–fusion experiment planned for the ELI-NP infrastructure. The simulations were performed using a fully relativistic multi-dimensional (2D3V) PIC code (Domański *et al.*, 2016, 2017) extended with "on-line" calculations of the ionization levels of the target atoms and accelerated ions that are of crucial importance for properly modeling the acceleration of super-heavy ions which are not fully ionized during the interaction with the laser pulse. For the investigated range of laser beam intensity, the dominant mechanism of ionization is tunneling ionization, and the Keldysh parameter for all ionization levels of thorium is much smaller than one. Furthermore, the ionization energies are much smaller than the electron rest energy (Popov, 2004; Kramida *et al.*, 2018). Thus, the process of ionization could be described using the Ammosov–Delone–Krainov formula (Ammosov *et al.*, 1986; Chen *et al.*, 2013), which was implemented in the code.

The simulations were performed for a circularly polarized 20 fs laser pulse with a wavelength equal to 0.8 μm, a peak intensity of $10^{23}$ W/cm$^2$ and a beam width (full width at half maximum) equal to 3 μm (these parameters correspond to a laser pulse energy of 150 J). The laser beam shape in time and space (along the $y$-axis) was described using a super-Gaussian function with a power index equal to 6. The source of Th ions was a flat thorium target with a thickness ($L_T$) equal to 50 or 200 nm, a transverse size of 12 μm and a molecular density corresponding to a solid-state density ($3 \times 10^{22}$ molecules/cm$^3$). A pre-plasma layer of 0.25 μm thick and with a density shape described by an exponential function was placed in front of the target.

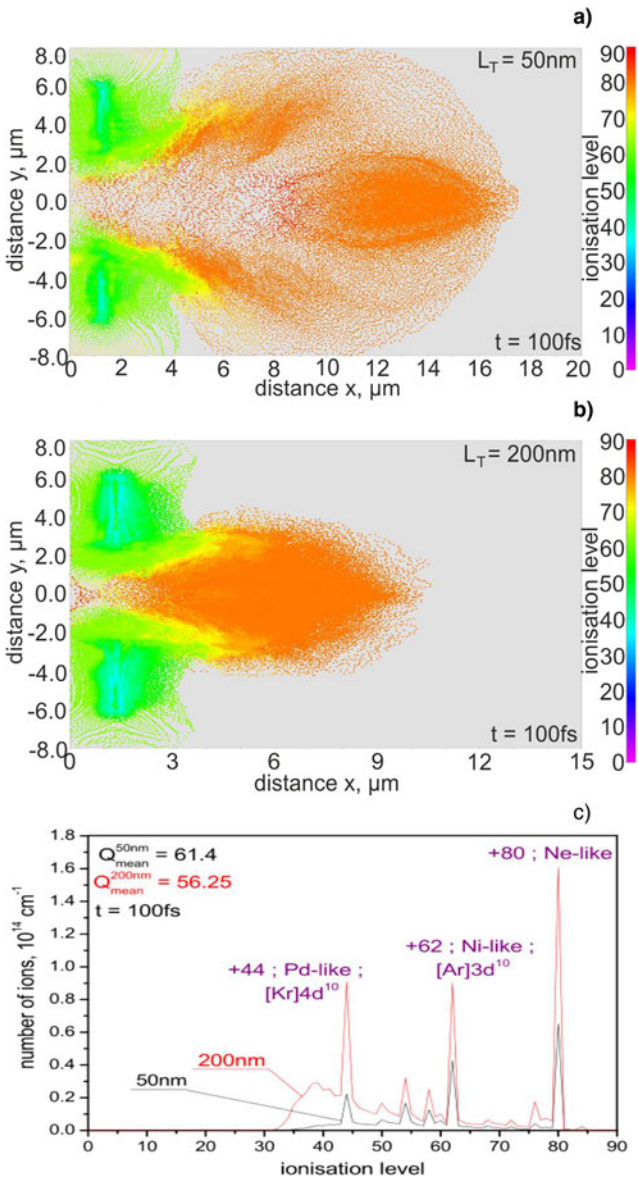


**Fig. 1.** The 2D spatial distributions of the average ionization level of thorium ions ($L_T$ = 50 nm – a, $L_T$ = 200 nm – b) and the comparison of the ionization spectra (c) for the two investigated targets.

## Results and discussion

A comparison of the ionization spectra for the two investigated thorium targets is shown in Figure 1c. The structure of both spectra is similar. Three main peaks are observed for both investigated targets, corresponding with the thorium ion ionization energy gap (Kramida *et al.*, 2018). The mean (averaged) ionization level is equal to 61.4 for the 50 nm target and 56.25 for the 200 nm target. The difference is only a few per cent and is the result of a higher number of ions with lower ionization levels in the thicker target. Figures 1a, 1b present the spatial (2D) distributions of the average ionization level of thorium ions for the two investigated targets. It is visible that the central regions of the targets (the main ion beams) are dominated by Ne-like thorium ions ($Th^{80+}$). The high ionization of the ions in the region of the laser–target interaction plays an important role in the stabilization of the ion acceleration process due to the increase in electron density in this

https://doi.org/10.1017/S0263034618000563 Published online by Cambridge University Press

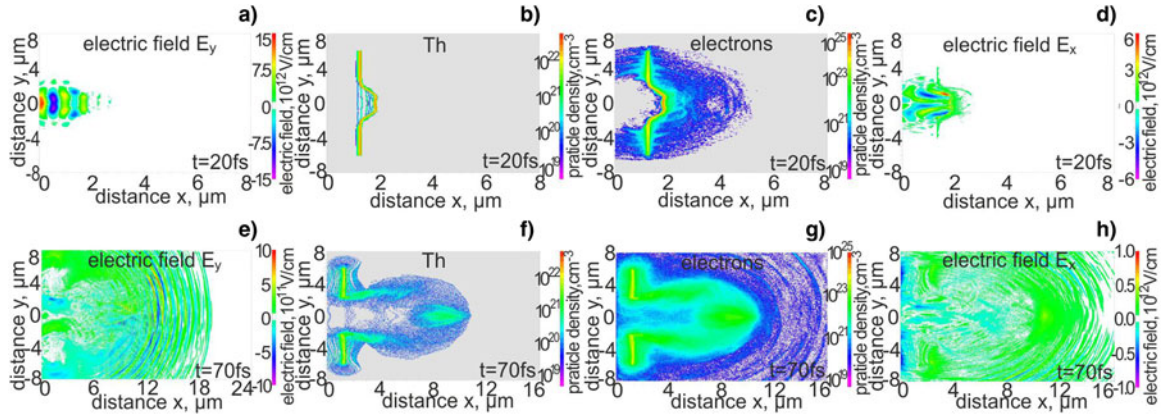


**Fig. 2.** The 2D spatial distribution of the electric field perpendicular to the laser beam axis $E_y$ (a, e), the particle density of thorium ions (b, f), the particle density of electrons (c, g), and the electric field in the plasma along the laser beam axis (d, h) at the simulation time $t = 20$ fs (a–d) and $t = 70$ ps (e–h). $L_T = 50$ nm.

region (Wu *et al.*, 2014). The ions with lower ionization levels occupy the edges of the targets. The lower ionization of the target edges reduce the efficiency of ion acceleration in this region. Due to the small difference in the average ionization levels for the 50 and 200 nm targets, this effect does not generate significant differences in the properties of ion beams generated from these targets.

Figure 2 presents the results obtained for the target of $L_T = 50$ nm, in particular the 2D spatial distribution of the electric field perpendicular to the laser beam axis $E_y$ (a, e), the particle density of thorium ions (b, f), the particle density of electrons (c, g), and the electric field in the plasma along the laser beam axis (d, h) at the simulation time $t = 20$ fs (a–d) comparable with the laser pulse duration and at the later stage of ion acceleration ($t = 70$ ps) (e–h) when the simulation time is several times longer than the laser pulse duration. At the first of the presented stages, a dense plasma bunch (with electrons moving together with ions) pushed forward by the radiation pressure of the laser pulse is visible (Figs 2b, 2c). This is a typical picture for the radiation pressure acceleration (RPA) acceleration mechanism, in particular for the light-sail (LS) stage, preceded by the hole-boring (HB) stage (Grech *et al.*, 2011; Daido *et al.*, 2012; Macchi *et al.*, 2013). This mechanism terminates when the direct interaction of the laser pulse with the target is terminated, that is, after a time comparable with the duration of the laser pulse. Despite this fact, the ions are still accelerated over a time much longer than the laser pulse duration (see Fig. 2h). At this stage, the dominant role in ion acceleration is played by the electric field generated by the fast electrons moving far away from the ions. On the edges of the target, the typical picture of the target normal sheath acceleration (TNSA) mechanism (Wilks *et al.*, 2001; Daido *et al.*, 2012; Macchi *et al.*, 2013; Wagner *et al.*, 2016) is visible, while in the center of the target (where the ions were accelerated by RPA) the sheath acceleration for the front surface of the plasma is noticeable.

Figure 3 presents results similar to those presented in Figure 2 but obtained for the target of $L_T = 200$ nm. Due to the higher thickness of the target, the RPA-HB stage lasts longer than for the thinner target (Fig. 3b) and the RPA-LS stage cannot develop since the laser pulse is too short. Also in this case, the post-RPA acceleration stage is observed (see Fig. 3h), though the sheath acceleration of ions for the thicker target is much weaker. Furthermore, despite the high ionization level in the interaction area (which results in high electron density), the 50 nm target becomes transparent for the laser light at the end of the RPA-stage (Fig. 2e) while the 200 nm target remains opaque for light (Fig. 3e).

For a better understanding of the ion acceleration process, the cross-section along the laser beam axis of the ion and electron charge density as well as the $E_x$ field for two time steps ($t = 20$ and $t = 70$ fs) and two investigated targets was prepared (Fig. 4). First of all, it is visible (Figs 4a, 4c) that during the RPA-stage of ion acceleration the TNSA mechanism also contributes to the acceleration process. However, the strength of the TNSA field depends on the target thickness. For the 50 nm target, the TNSA field reaches a value of 2.0 TV/cm (for $t = 20$ fs, Fig. 4a) and is comparable with the RPA field, while for the thicker target it reaches only 500 GV/cm (Fig. 4c) and is more than five times lower than the RPA field. The difference in ion acceleration efficiency for the two considered targets is also clearly visible in the post-RPA stage ($t = 70$ fs, Figs 4b, 4d). The sheath acceleration field for the 50 nm target reaches the value of 350 GV/cm (Fig. 4b), while for the 200 nm target it reaches only 90 GV/cm (Fig. 4d). The lower efficiency of TNSA and sheath acceleration for the thicker target results from the lower temperature of electrons for this target (the accelerating field $E_{ac} = T_h/e\lambda_{Dh}$, where $T_h$ is the hot electron temperature and $\lambda_{Dh}$ is the Debye length) (Macchi *et al.*, 2013). The amount of laser-produced hot electrons in the 200 nm target is higher than that in the 50 nm target and, as a result, the energies and temperatures achieved by the electrons in the thicker target are lower (the mean electron energy at $t = 70$ fs is equal to 14.9 MeV for the 50 nm target and 2.89 MeV for the 200 nm target).

Figure 5 presents the energy spectra of thorium ions and the temporal shapes of the ion pulse for both types of investigated targets.

Figure 5a shows the energy spectra for the end of the ion acceleration process ($t = 150$ fs). It is clear that for both targets the ion energy spectra are broad, but the 50 nm target shows a noticeable peak in the spectrum around 30 GeV. The occurrence of this peak could be explained by the presence of the RPA-LS stage in the ion acceleration process in the case of the thinner target. Unfortunately, the strong sheath acceleration during the post-RPA stage destroys the potentially quasi-monochromatic spectrum. For the thicker target, the sheath acceleration mechanism is much weaker, but the light sail stage of acceleration is not present, which negatively influences the quality of the ion

https://doi.org/10.1017/S0263034618000563 Published online by Cambridge University Press

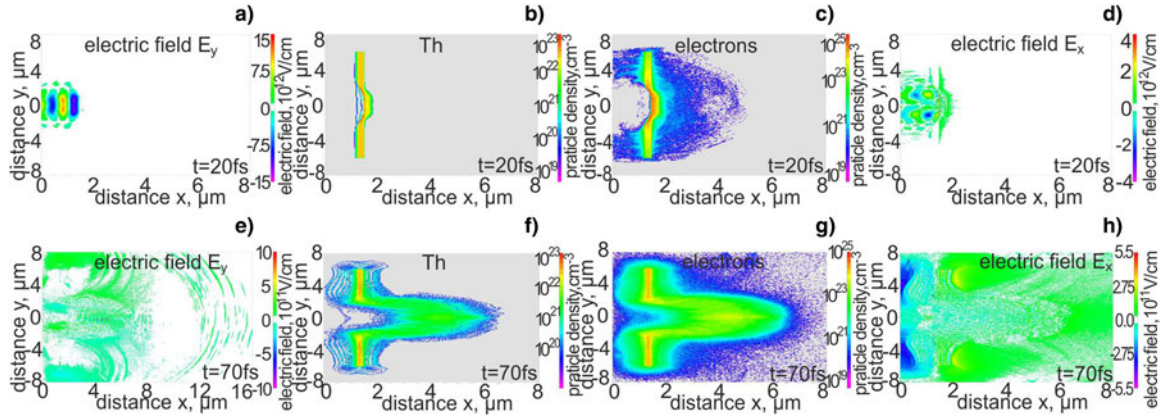


**Fig. 3.** The 2D spatial distribution of the electric field perpendicular to the laser beam axis $E_y$ (a, e), the particle density of thorium ions (b, f), the particle density of electrons (c, g), and the electric field in the plasma along the laser beam axis (d, h) at the simulation time $t = 20$ fs (a–d) and $t = 70$ ps (e–h). $L_T = 200$ nm.

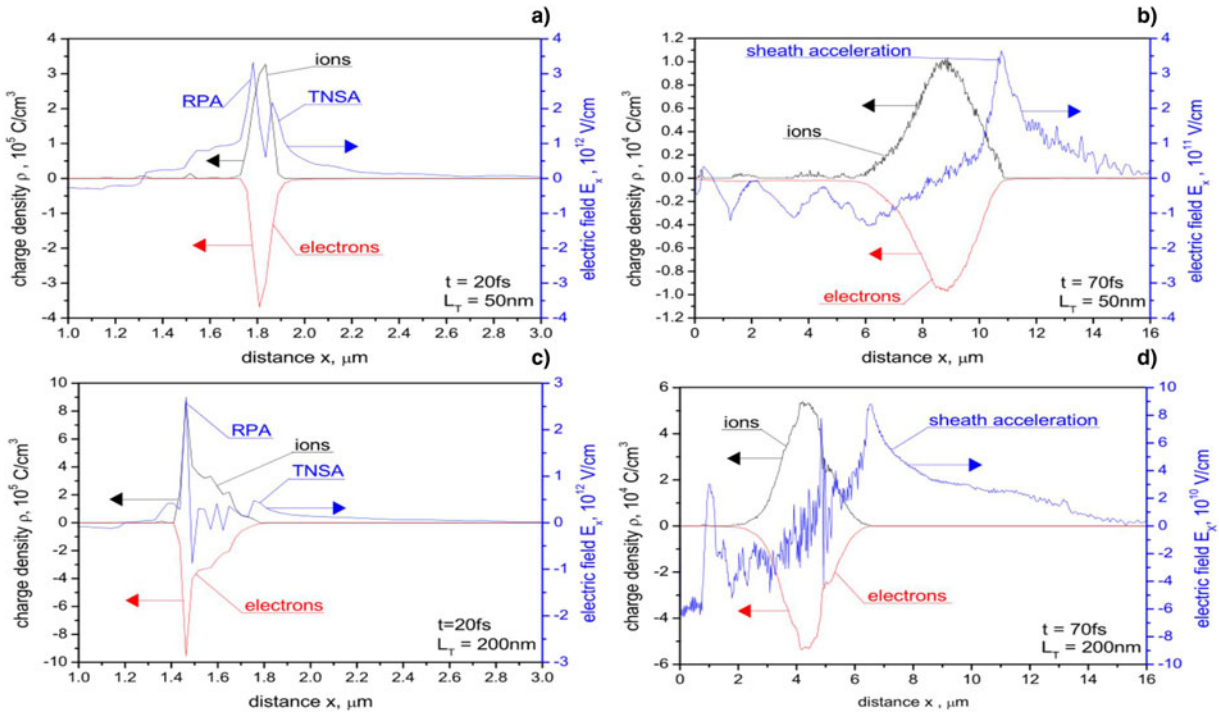


**Fig. 4.** The cross-section along the laser beam axis of the ion and electron charge density as well as the $E_x$ field for two time steps [$t = 20$ fs (a, c) and $t = 70$ fs (b, d)] and two investigated targets [$L_T = 50$ nm (a, b) and $L_T = 200$ nm (c, d)].

energy spectrum. As could be expected, both mean and maximum ion energies are higher for the thinner target. The mean energy is equal to 19.3 GeV (83 MeV/nucleon) for the 50 nm target and 2.49 GeV (11 MeV/nucleon) for the 200 nm target. Both of the values are higher than the 7 MeV/nucleon required for the proposed fission–fusion reaction mechanism (Negoita *et al.*, 2016). The maximum ion energy reaches a value of around 20 GeV (86 MeV/nucleon) for the thicker target and ~100 GeV (431 MeV/nucleon) for the thinner target.

Figure 5b presents a comparison of the temporal shapes of the thorium ion beams generated from the central region of the investigated targets and recorded 20 μm behind the target. Although the energy spectra of thorium ions are broad, the ion pulse durations are in the femtosecond range and the peak intensities of the ion pulses reach extremely high values above $10^{21}$ W/cm$^2$. The intensities of the pulses are very high because the ion bunches are dense, and the ions in the bunches have high energies (the intensity $I_i = n_i v_i E_i$, where $n_i$, $v_i$, and $E_i$ are the ion density, velocity, and energy, respectively). Furthermore, the ion pulse for the thinner target is more intense and shorter than the ion pulse for the thicker target. The peak intensity of the ion pulse reaches the value of $8 \times 10^{21}$ W/cm$^2$ for the 50 nm target and $1 \times 10^{21}$ W/cm$^2$ for the 200 nm target. Those values are a factor of $10^2$ higher than the ion beam intensities available currently in conventional RF-driven ion acceleration, and higher than the $10^{20}$ W/cm$^2$ value required for the fission–fusion reaction mechanism (Negoita *et al.*, 2016).

The number of accelerated thorium ions and the ion fluence for the central region of the investigated targets are presented in

https://doi.org/10.1017/S0263034618000563 Published online by Cambridge University Press

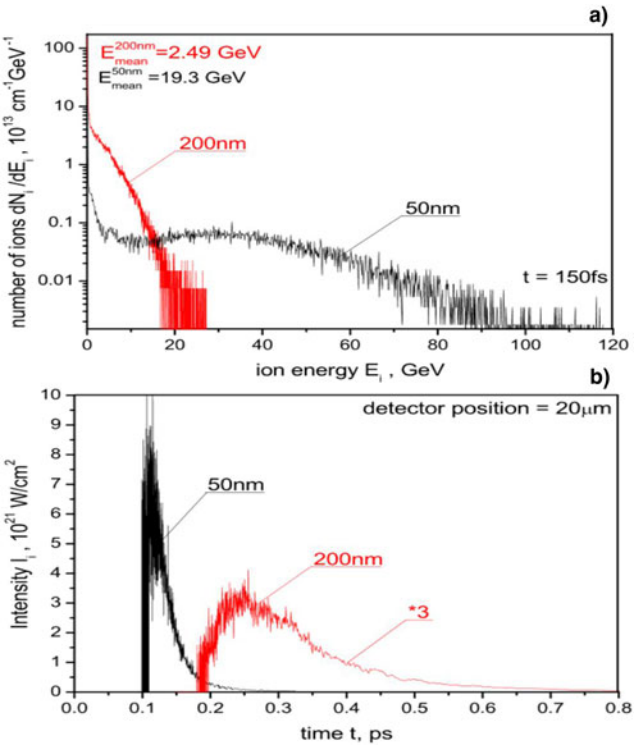


**Fig. 5.** The energy spectra of thorium ions (a) and the temporal shapes of the ion pulse (b) for both types of investigated targets and for the central region of a target with diameter $D_c = 6$ μm.

Table 1. It is visible that the values of $N_i$ and $F_i$ for the 200 nm target are higher than for the thinner one, and are fairly close to those postulated for the fission–fusion experiment at ELI-NP.

For very high laser intensities ~$10^{23}$ W/cm$^2$ or higher, the process of ion acceleration can potentially be accompanied by the production of ultra-relativistic electrons of the Lorentz factor $\gamma \gg 1$. Such electrons, with an energy equal to tens of MeV or higher, can lose part of their energy due to synchrotron radiation. These radiation losses (RL) can influence the process of ion acceleration (Schlegel *et al.*, 2009; Tamburini *et al.*, 2010; Capdessus and McKenna, 2015). The influence of RL on the acceleration process significantly depends on the parameters of laser pulse and the target. In contrast to the proton and deuterons considered in Schlegel *et al.* (2009), Tamburini *et al.* (2010), and Capdessus and McKenna (2015), thorium ions achieve non-relativistic velocities even for laser pulse intensities equal to $10^{23}$ W/cm$^2$. Due to the high charge state of the thorium ions and the circular polarization (Tamburini *et al.*, 2010) of the laser pulse, a vast majority of the accelerated electrons are strongly coupled to these (non-relativistic) ions (Figs 2 and 3). For this reason, the electron energies are relatively small. For the 50 nm target 2.7% of electrons achieve ultra-relativistic energies (>50 MeV) and for the 200 nm target just 0.01% of electrons achieve such energies. Therefore, the case of ion acceleration investigated in our paper is essentially different from the cases considered in Schlegel *et al.* (2009), Tamburini *et al.* (2010), and Capdessus and McKenna (2015), and it is reasonable to believe that the influence of RL on the ion beam parameters is small for the 50 nm target and negligible for the 200 nm one.

The investigations of the laser-driven acceleration of super-heavy ions presented in this paper are focused on the acceleration of thorium ions. However, the main conclusions drawn from these investigations can be considered valid for other super-heavy ions such as gold, lead, or uranium ions. This is due to the fact that the ion acceleration process depends mainly on the $q/m$ parameter, which is similar for all super-heavy ions ($q$ is the ion charge and $m$ is the ion mass). The heavier atoms are easier to ionize to higher levels, and the difference in $q/m$ parameters between the various super-heavy ions is even smaller than results from their masses only. As a result, the differences between the processes of acceleration of super-heavy ions like Au, Pb, Th, or U ions are expected to be small. This conclusion was proven by the results of our additional PIC simulations, which we carried out for Pb ions and compared with the results for Th ions.

**Table 1.** The number of accelerated ions and the ion fluence for the central region of a target with diameter $D_c = 6$ μm

| | Number of ions $N_i$ | Ion fluence $F_i$, cm$^{-2}$ |
|---|---|---|
| 50 nm target | $3.2 \times 10^{10}$ | $9.4 \times 10^{16}$ |
| 200 nm target | $1.5 \times 10^{11}$ | $5.0 \times 10^{17}$ |

## Summary and conclusions

In summary, the acceleration of super-heavy ($A > 200$) ions from sub-micrometer thorium targets irradiated by a multi-PW fs laser pulse of ultra-relativistic intensity has been investigated with the use of a relativistic 2D3V PIC code, supplemented with "on-line" calculations of the ionization of the target atoms and accelerated thorium ions. It has been found that the acceleration process of super-heavy ions at ultra-relativistic laser intensities is fairly complex, and in this process the RPA stage is followed by a sheath acceleration stage, with a significant role in the second stage being played by the ballistic movement of ions accelerated at the RPA stage. The detailed run of the acceleration process depends on the target thickness. In the case of a thicker target (here 200 nm thick), the average ionization level of the target is lower than that in the case of a thinner target (here 50 nm thick), the mean energies (temperatures) of laser-produced hot electrons are lower as well, and the ions acquire the vast majority of their energy at the RPA-HB stage of acceleration. In the case of a thinner target, the mean energies of hot electrons are higher and the sheath acceleration plays a more important role in the acceleration process, with a significant part of the ion energies being acquired in the post-RPA stage. In addition, since the number of accelerated ions is lower in this case, both the mean and maximum ion energy is higher for the thicker target. The existence of the sheath acceleration stage of ion acceleration seems to be the main reason why the energy spectrum of accelerated ions is wide in the cases of both a thinner and thicker target.

Despite the wide energy spectrum of the accelerated ions, the produced ion beams are very short and extremely intense. It has been demonstrated that the 20-fs, 150-J laser pulse with an intensity of ~$10^{23}$ W/cm$^2$ to be generated by the multi-PW ELI-NP laser is capable of producing a sub-ps thorium ion beam with ~$10^{11}$ ions of GeV energies, an ion beam intensity >$10^{21}$ W/cm$^2$ and an ion fluence ~$10^{17}$–$10^{18}$ ions/cm$^2$. The last two values are much higher than attainable in conventional accelerators, and are fairly promising for the planned ELI-NP experiments. Such very intense, ultra-short heavy ion beams provide the prospect for innovative applications of these beams not only in nuclear physics, but also in HEDP and possibly in other fields of research.

https://doi.org/10.1017/S0263034618000563 Published online by Cambridge University Press

**Acknowledgments.** This work has been carried out in part within the framework of the EUROfusion Consortium and has received partial funding from the Euratom research and training programme 2014–2018 under grant agreement no. 633053. The views and opinions expressed herein do not necessarily reflect those of the European Commission. The simulations were carried out with the support of the Interdisciplinary Centre for Mathematical and Computational Modelling (ICM), University of Warsaw under grant no. G57-20.

## References

**Ammosov MV, Delone NB and Krainov VP** (1986) Tunnel ionization of complex atoms and of atomic ions in an alternating electromagnetic field. *Journal of Experimental and Theoretical Physics* **64**, 1191.

**Badziak J, Parys P, Vankov AB, Wołowski J and Woryna E** (2001). Generation of fluxes of highly charged ions from a picosecond laser-produced plasma. *Applied Physics Letters* **79**, 21–23.

**Badziak J, Hora H, Woryna E, Jabłoński S, Laska L, Parys P, Rohlena K and Wołowski J** (2003). Experimental evidence of differences in properties of fast ion fluxes from short-pulse and long-pulse laser-plasma interactions. *Physics Letters A* **315**, 452–457.

**Capdessus R and McKenna P** (2015). Influence of radiation force on ultraintense laser-driven ion acceleration. *Physical Review E* **91**, 053105.

**Chen M, Cormier-Michel E, Geddes CGR, Bruhwiler DL, Yu LL, Esarey E, Schroeder CB and Leemans WP** (2013). Numerical modelling of laser tunnelling ionization in explicit particle-in-cell codes. *Journal of Computational Physics* **236**, 220.

**Clark EL, Krushelnick K, Zepf M, Beg FN, Tatarakis M, Machacek A, Santala MIK, Watts I, Norreys PA and Dangor AE** (2000). Energetic heavy-ion and proton generation from ultraintense laser-plasma interactions with solids. *Physical Review Letters* **85**, 1654–1657.

**Daido H, Nishiuchi M and Pirozhkov AS** (2012). Review of laser-driven ion sources and their applications. *Reports on Progress in Physics* **75**, 056401.

**Danson C, Hillier D, Hopps N and Neely D** (2015). Petawatt class lasers worldwide. *High Power Laser Science Engineering* **3**, e3.

**Domański J, Badziak J and Jabłoński S** (2016). Enhanced efficiency of femtosecond laser-driven proton generation from a two-species target with heavy atoms. *Laser and Particle Beams* **34**, 294.

**Domański J, Badziak J and Jabłoński S** (2017). Generation of proton beams from two-species targets irradiated by a femtosecond laser pulse of ultrarelativistic intensity. *Laser and Particle Beams* **35**, 286.

**Flippo K, Hegelich BM, Albright BJ, Yin L, Gautier DC, Letzring S, Schollmeier M, Schreiber J, Schulze R and Fernandez JC** (2007). Laser-driven ion accelerators: Spectral control, monoenergetic ions and new acceleration mechanisms. *Laser and Particle Beams* **25**, 3.

**Grech M, Skupin S, Diaw A, Schlegel T and Tikhonchuk VT** (2011). Energy distribution in radiation pressure accelerated ion beams. *New Journal of Physics* **13**, 123003.

**Hoffmann DHH, Fortov VE, Kuster M, Mintsev V, Sharkov BY, Tahir NA, Udrea S, Varentsov D and Weyrich K** (2009). High energy density physics generated by intense heavy ion beams. *Astrophysics and Space Science* **322**, 167.

**Kramida A, Ralchenko Yu and Reader J, NIST ASD Team** (2018). *NIST Atomic Spectra Database* (ver. 5.5.6), [Online]. Available: https://physics.nist.gov/asd [2018, August 2]. National Institute of Standards and Technology, Gaithersburg, MD.

**Macchi A, Borghesi M and Passoni M** (2013). Ion acceleration by superintense laser–plasma interaction. *Reviews of Modern Physics* **85**, 751.

**McKenna P, Ledingham KWD, Yang JM, Robson L, McCanny T, Shimizu S, Clarke RJ, Neely D, Spohr K, Chapman R, Singhal RP, Krushelnick K, Wei MS and Norreys PA** (2004). Characterization of proton and heavier ion acceleration in ultrahigh-intensity laser interactions with heated target foils. *Physical Review E* **70**, 036405.

**Negoita F, Roth M, Thirolf PG, Tudisco S, Hannachi F, Moustaizis S, Pomerantz I, McKenna P, Fuchs J, Sphor K, Acbas G, Anzalone A, Audebert P, Balascuta S, Cappuzzello F, Cernaianu MO, Chen S, Dancus I, Freeman R, Geissel H, Ghenuche P, Gizzi L, Gobet F, Gosselin G, Gugiu M, Higginson D, D'Humieres E, Ivan C, Jaroszynski D, Kar S, Lamia L, Leca V, Neagu L, Lanzalone G, Meot V, Mirfayzi SR, Mitu IO, Morel P, Murphy C, Petcu C, Petrascu H, Petrone C, Raczka P, Risca M, Rotaru F, Santos JJ, Schumacher D, Stutman D, Tarisien M, Tataru M, Tatulea B, Turcu ICE, Versteegen M, Ursescu D, Gales S and Zamfir NV** (2016). Laser driven nuclear physics at ELI-NP. *Romanian Reports in Physics* **68**, S37.

**Nishiuchi M, Sakaki H, Esirkepov TZh, Nishio K, Pikuz TA, Faenov AYa, Skobelev IYu, Orlandi R, Sako H, Pirozhkov AS, Matsukawa K, Sagisaka A, Ogura K, Kanasaki M, Kiriyama H, Fukuda Y, Koura H, Kando M, Yamauchi T, Watanabe Y, Bulanov SV, Kondo K, Imai K and Nagamiya S** (2015). Acceleration of highly charged GeV Fe ions from a low-Z substrate by intense femtosecond laser. *Physics of Plasmas* **22**, 033107.

**Petrov GM, McGuffey C, Thomas AGR, Krushelnick K and Beg FN** (2016). Generation of heavy ion beams using femtosecond laser pulses in the target normal sheath acceleration and radiation pressure acceleration regimes. *Physics of Plasmas* **23**, 063108.

**Popov VS** (2004). Tunnel and multiphoton ionization of atoms and ions in a strong laser field (Keldysh theory). *Physics-Uspekhi* **47**, 855.

**Schlegel T, Naumova N, Tikhonchuk VT, Labaune C, Sokolov IV and Mourou G** (2009). Relativistic laser piston model: Ponderomotive ion acceleration in dense plasmas using ultraintense laser pulse. *Physics of Plasmas* **16**, 083103.

**Sharkov BYu, Hoffmann DHH, Golubev AA and Yongtao Z** (2016). High energy density physics with intense ion beams. *Matter Radiation Extremes* **1**, 28.

**Tamburini M, Pegoraro F, Di Piazza A, Keitel CH and Macchi A** (2010). Radiation reaction effects on radiation pressure acceleration. *New Journal of Physics* **12**, 123005.

**Wagner F, Brabetz C, Deppert O, Roth M, Stöhlker T, Tauschwitz An, Tebartz A, Zielbauer B and Bagnoud V** (2016). Accelerating ions with high-energy short laser pulses from submicrometer thick targets. *High Power Laser Science and Engineering* **4**, e45.

**Wilks SC, Langdon AB, Cowan TE, Roth M, Singh M, Hatchett S, Key MH, Pennington D, MacKinnon A and Snavely RA** (2001). Energetic proton generation in ultra-intense laser-solid interactions. *Physics of Plasmas* **8**, 542.

**Wu D, Qiao B, McGuffey C, He XT and Beg FN** (2014). Generation of high-energy mono-energetic heavy ion beams by radiation pressure acceleration of ultra-intense laser pulses. *Physics of Plasmas* **21**, 123118. www.eli-laser.eu

https://doi.org/10.1017/S0263034618000563 Published online by Cambridge University Press